

The Dynamics of Coupled Spin-Torque Nano Oscillators: An Initial Exploration

J. Turtle, A. Palacios, V. In and P. Longhini

Abstract In this work we explore the use of Spin Torque Nano Oscillators (STNOs) to produce a spintronics voltage oscillator in the microwave range. STNOs are quite small—on the order of 10 nm—and frequency agile. However, experimental results to date have produced power outputs that are too small to be viable. We attempt to increase power output by investigating the dynamics of a system of electrically-coupled STNOs. To set the foundation for further analysis, we consider both Spherical and Complex Stereographic coordinates for the Landau-Lifshitz-Gilbert Equation with spin torque term. Both coordinate systems effectively reduce the equation of a single STNO from three dimensions to two. Further, the Complex Stereographic representation transforms the equation into a nearly polynomial form that may prove useful for advanced dynamics analysis. Qualitative bifurcation diagrams show a rich set of behaviors in the parallel and series coupled systems and serve to develop intuition in system dynamics.

1 Introduction

Spin Torque Nano Oscillators (STNO) are a ferromagnet-based electronics component. In certain steady-states, the magnetic moment precesses causing component resistance to oscillate [1]. Based on this oscillating resistance, an STNO can be utilized as a microwave-range voltage oscillator (see Fig. 1). STNOs offer many potential advantages over existing semi-conductor voltage oscillators including small physical size (~ 10 nm), a large tunable frequency range, and small output linewidths [2]. However, STNOs tested to date have yet to produce adequate power. STNOs need

J. Turtle · A. Palacios (✉) · V. In · P. Longhini
San Diego State University, San Diego, CA 2182, USA
e-mail: jturtle@rohan.sdsu.edu

A. Palacios
e-mail: apalacios@mail.sdsu.edu

to output at least 1 mW to be applicable [3]. The microwave power generated by an STNO was first measured in 2009 on the order of 100 nW [4]. STNOs cannot be made larger, so an obvious solution to increasing power is to couple multiple oscillators. However, in experiments it has proven difficult to synchronize even two STNOs [5]. Thus we have begun to study the dynamics of coupled STNOs to determine conditions for synchronization. In this article we report our initial findings starting with the model itself. We first explore alternate coordinate systems to reduce the dimension of the model and find a form that is more amenable to later analysis. Both spherical and complex stereographic coordinates are investigated. Next we vary the input current and numerically integrate until steady-state to create qualitative bifurcation diagrams. Bifurcation diagrams are generated for both parallel and series connected STNOs.

2 The Model

Magnetization in the free ferromagnetic layer is described by the Landau-Lifshitz equation with Gilbert damping and Slonczewski-Berger spin-torque term (LLGS) [6–10]

$$\frac{d\mathbf{m}}{dt} = \underbrace{-\gamma \mathbf{m} \times \mathbf{H}_{\text{eff}}}_{\text{precession}} + \underbrace{\lambda \mathbf{m} \times \frac{d\mathbf{m}}{dt}}_{\text{damping}} - \underbrace{\gamma a g (P, \mathbf{m} \cdot \mathbf{S}_p) \mathbf{m} \times (\mathbf{m} \times \mathbf{S}_p)}_{\text{spin transfer torque}}, \quad (1)$$

where \mathbf{m} represents the magnetization of the free ferromagnetic layer in Cartesian coordinates, γ is the gyromagnetic ratio and \mathbf{H}_{eff} is the effective field. λ serves as the magnitude of the damping term. In the spin torque term, a has units Oe and is proportional to the electrical current density [11]. g is a function of the polarization factor P , \mathbf{m} , and the fixed-layer magnetization direction \mathbf{S}_p . To determine the change of field direction with respect to time, we must consider three different classes of torques acting on the field direction \mathbf{m} : effective external magnetic field \mathbf{H}_{eff} , damping λ , and spin transfer torque. \mathbf{H}_{eff} is the sum of several factors that can be effectively represented as external fields. The factors that we consider in this fashion are exchange, anisotropy and demagnetization. The actual external, or applied, field rounds out the sum

$$\mathbf{H}_{\text{eff}} = \mathbf{H}_{\text{exchange}} + \mathbf{H}_{\text{anisotropy}} + \mathbf{H}_{\text{demagnetization}} + \mathbf{H}_{\text{applied}}.$$

We model the free layer as a single particle who's magnetization \mathbf{m} represents the average of the layer. Thus there is no exchange with adjacent magnetic moments $\mathbf{H}_{\text{exchange}} = \mathbf{0}$.

Spherical Coordinates

In Eq. (1), \mathbf{m} has constant magnitude. We confine \mathbf{m} to the surface of a unit sphere by choosing $\|\mathbf{m}\|_2 = 1$. Thus, spherical coordinates are a natural choice for \mathbf{m} with the radius $\rho = 1$. In [12], Sun showed that Eq. (1) can be converted to

$$\begin{aligned} \frac{d\theta}{d\tau} = & -\alpha \sin \theta \cos \theta \\ & - h_p [(\sin \varphi + \alpha \cos \varphi) \sin \theta \cos \varphi] \\ & - h [\cos \varphi \sin \psi + \alpha (\sin \theta \cos \psi - \cos \theta \sin \varphi \sin \psi)] \\ & + h_s [\alpha \cos \varphi \sin \phi + \sin \varphi \sin \phi \cos \theta - \cos \phi \sin \theta], \end{aligned} \quad (2)$$

$$\begin{aligned} \frac{d\varphi}{d\tau} = & -\cos \theta \\ & - h_p [(\cos \varphi \cos \theta - \alpha \sin \varphi) \cos \varphi] \\ & - h \left[\frac{\sin \theta \cos \psi - \cos \theta \sin \varphi \sin \psi - \alpha \cos \varphi \sin \psi}{\sin \theta} \right] \\ & + h_s \left[\frac{\cos \varphi \sin \phi - \alpha \sin \varphi \sin \phi \cos \theta}{\sin \theta} + \alpha \cos \phi \right], \end{aligned}$$

where θ is the angle of inclination and φ is the azimuthal angle. These equations have been time-scaled by $\frac{\gamma h_k}{1+\lambda^2}$ (h_k is the magnitude of anisotropy) and parameters consolidated to: demagnetization magnitude h_p (yz -easy-plane), applied field magnitude h , applied field angle from z -axis ψ (confined to yz -plane), spin torque magnitude h_s , and spin torque angle from z -axis ϕ (also confined to yz -plane). Ultimately reducing the representation of the system from three dimensions to two.

Complex Stereographic Projection

A spherical surface can be projected onto a plane by using the complex variable ω and the following relationships:

$$\omega = \frac{m_x + im_y}{1 + m_z} \Rightarrow \mathbf{m} = \begin{bmatrix} \frac{\omega + \bar{\omega}}{1 + |\omega|^2} \\ -i \frac{(\omega - \bar{\omega})}{1 + |\omega|^2} \\ \frac{1 - |\omega|^2}{1 + |\omega|^2} \end{bmatrix}. \quad (3)$$

Building on [11, 13], we reduce Eq. (1) to the form

$$\begin{aligned} \dot{\omega} = & \frac{\gamma}{1 - i\lambda} \left(-a\omega + ih_{a3}\omega + \frac{h_{a2}}{2}(1 + \omega^2) \right. \\ & \left. + im_{\parallel}\kappa \left[\cos\theta_{\parallel}\omega - \frac{1}{2}\sin\theta_{\parallel} \left(e^{i\phi_{\parallel}} - \omega^2 e^{-i\phi_{\parallel}} \right) \right] \right. \\ & - \frac{i4\pi S_0}{(1 + |\omega|^2)} \left[N_3(1 - |\omega|^2)\omega - \frac{N_1}{2}(1 - \omega^2 - |\omega|^2)\omega \right. \\ & \left. \left. - \frac{N_2}{2}(1 + \omega^2 - |\omega|^2)\omega - \frac{(N_1 - N_2)}{2}\bar{\omega} \right] \right), \end{aligned} \tag{4}$$

where h_{a2} is the magnitude of the applied field in the y -direction and h_{a3} is the magnitudes of the applied field in the z -direction. κ is the anisotropy magnitude who's direction is determined by θ_{\parallel} and ϕ_{\parallel} . The anisotropy is scaled by $m_{\parallel} = \mathbf{m} \cdot \mathbf{e}_{\parallel}$ where

$$\mathbf{e}_{\parallel} = \begin{bmatrix} \sin\theta_{\parallel} \cos\phi_{\parallel} \\ \sin\theta_{\parallel} \sin\phi_{\parallel} \\ \cos\theta_{\parallel} \end{bmatrix}.$$

S_0 is the saturation magnetization. Finally, $N_1 + N_2 + N_3 = 1$ and determine the effective demagnetization field resulting from the shape of the free layer. Now we have a two dimensional expression for the STNO that is close to polynomial form.

Coupling

Coupling is achieved by modeling a simple electrical circuit with STNOs arrayed in series or parallel. Figure 1 depicts the series configuration. The resistance of each STNO R_i is a function of the angle θ_i between M (fixed layer-green) and \mathbf{m} (free layer-red):

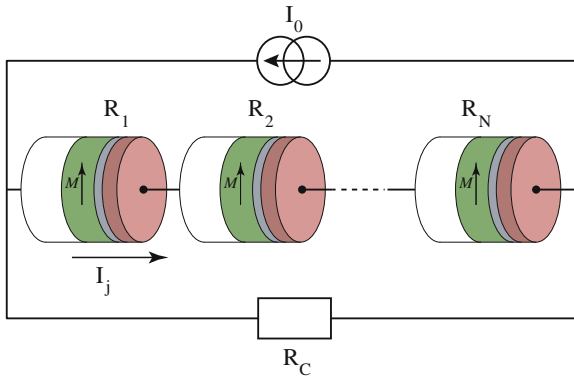


Fig. 1 Series arrayed STNOs with input current I_0 and output resistance R_C

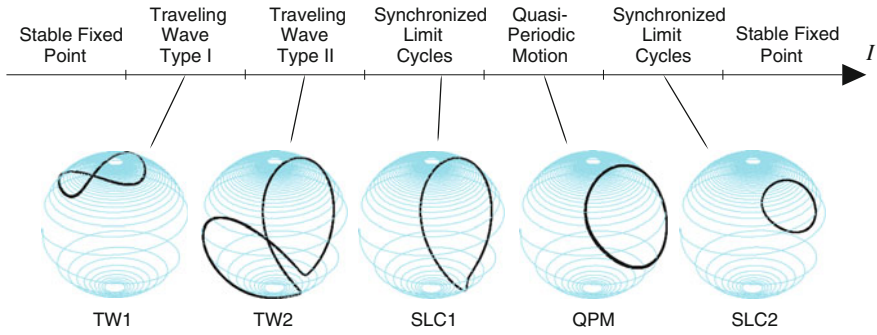


Fig. 2 Qualitative bifurcation diagram for 3 STNOs arranged in series and varying parameter I over the interval [0:3]

$$R_i = R_{0i} - \Delta R_i \cos \theta_i.$$

Here, R_0 is the median resistance of an STNO and ΔR is the maximum variance in resistance.

3 Numerical Exploration

Numeric simulations have revealed a rich variety of behaviors in a series-array of three STNOs. Figure 2 depicts a few example behaviors found by varying the current I . A high or low current simply causes all of the oscillators to converge to an equilibrium point. However, in the intermediate range there are multiple distinct regimes of oscillatory behavior. All numeric integrations in this diagram use the parameters: $\lambda = 0.1$, $h = 1$, $h_s = -1$, $h_p = 5$, $\phi = 0$, $\psi = \pi/4$, $R_0 = 2$, $\Delta R = 0.6$, $R_c = 50$.

Performing similar integrations for 3 STNOs coupled in parallel generates the qualitative bifurcation diagram in Fig. 3. As is seen, we find a region of oscillations in I bound on both sides by fixed points. Within the oscillatory region we discovered six distinct sub-regions. Three sub regions tend to synchronization, two show quasi-periodic motion, and one forms frequency synchronized orbits. All numeric integrations in this diagram use the parameters: $\lambda = 0.1$, $h = 1$, $h_s = -1$, $h_p = 5$, $\phi = 0$, $\psi = \pi/4$, $R_0 = 0.1$, $\Delta R = 0.03$, $R_c = 50$.

4 Remarks

The LLGS Eq. (1) is a nonlinear first-order ordinary differential equation confined to the unit sphere $\|\mathbf{m}\|_2 = 1$. We are able to reduce the dimension of a system of coupled STNOs by one-third using spherical or complex-stereographic coordinates.

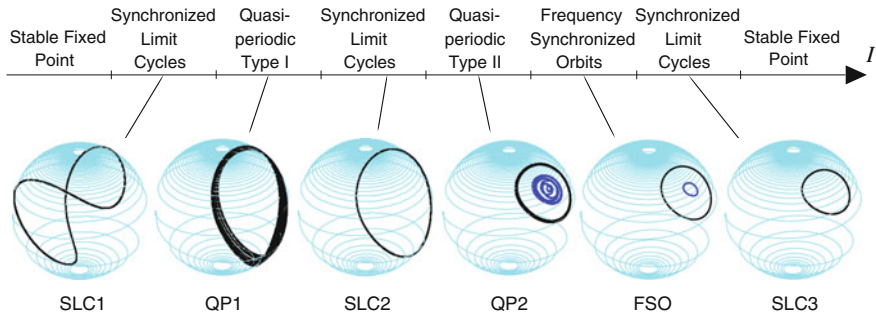


Fig. 3 Qualitative bifurcation diagram for 3 STNOs arranged in parallel and varying parameter I over the interval $[0;7]$

Not only does this increase the efficiency of numerics, but will also help in the future with a center manifold reduction. Furthermore, the form of the equations in complex stereographic coordinates is polynomial-like which may be helpful in future analysis.

In the series and parallel electric coupling scenarios, the system experiences all-to-all coupling or S_N symmetry. Most of the non-synchronous oscillating behaviors observed in Figs. 2 and 3 are consistent with $S_N \times S^1$ symmetry-breaking Hopf bifurcations. This leads us to believe that we can leverage the work of [14] to determine the existence and stability of non-synchronous oscillations.

References

1. A. Slavin, V. Tiberkevich, Nonlinear auto-oscillator theory of microwave generation by spin-polarized current. *IEEE T. Magn.* **45**(4), 1875–1918 (2009)
2. W. Rippard, M. Pufall, S. Russek, Comparison of frequency, linewidth, and output power in measurements of spin-transfer nanocontact oscillators. *Phys. Rev. B* **74**(22), 224, 409 (2006)
3. J. Persson, Y. Zhou, J. Akerman, Phase-locked spin torque oscillators: impact of device variability and time delay. *J. Appl. Phys.* **101**(9), 09A503–09A503 (2007)
4. A.E. Wickenden, C. Fazi, B. Huebschman, R. Kaul, A.C Perrella, W.H. Rippard, M.R. Pufall, Spin torque nano oscillators as potential terahertz (THz) communications devices. Tech. rep., DTIC Document (2009)
5. D. Li, Y. Zhou, C. Zhou, B. Hu, Global attractors and the difficulty of synchronizing serial spin-torque oscillators. *Phys. Rev. B* **82**(14), 140, 407 (2010)
6. L. Berger, Emission of spin waves by a magnetic multilayer traversed by a current. *Phys. Rev. B* **54**(13), 9353–9358 (1996). doi:[10.1103/PhysRevB.54.9353](https://doi.org/10.1103/PhysRevB.54.9353)
7. G. Bertotti, I. Mayergoyz, C. Serpico, Analytical solutions of Landau-Lifshitz equation for precessional dynamics. *Phys. B* **343**(1–4), 325–330 (2004)
8. M. d’Aquino, Nonlinear magnetization dynamics in thin-films and nanoparticles. Ph.D. thesis, Università degli Studi di Napoli Federico II, Naples (2004)
9. T. Gilbert, A phenomenological theory of damping in ferromagnetic materials. *IEEE T. Magn.* **40**(6), 3443–3449 (2004)
10. J.C. Slonczewski, Current-driven excitation of magnetic multilayers. *J. Magn. Magn. Mater.* **159**(1–2), L1–L7 (1996)

11. S. Muruges, M. Lakshmanan, Spin-transfer torque induced reversal in magnetic domains. *Chaos Solitons Fractals* **41**, 2773–2781 (2009)
12. J.Z. Sun, Spin-current interaction with a monodomain magnetic body: a model study. *Phys. Rev. B* **62**, 570–578 (2000)
13. S. Muruges, M. Lakshmanan, Bifurcation and chaos in spin-valve pillars in a periodic applied magnetic field. *Chaos* **19**, 043, 111 (2009)
14. A.P.S. Dias, A. Rodrigues, Hopf bifurcation with sn-symmetry. *Nonlinearity* **22**(3), 627 (2009)